Liquid sunshine

Drizzle, showers and torrential rain on the Sun

It is cold (relatively), dense and it moves through the solar corona. Seray Şahin and Patrick Antolin try to make sense of the enigma that is coronal rain.

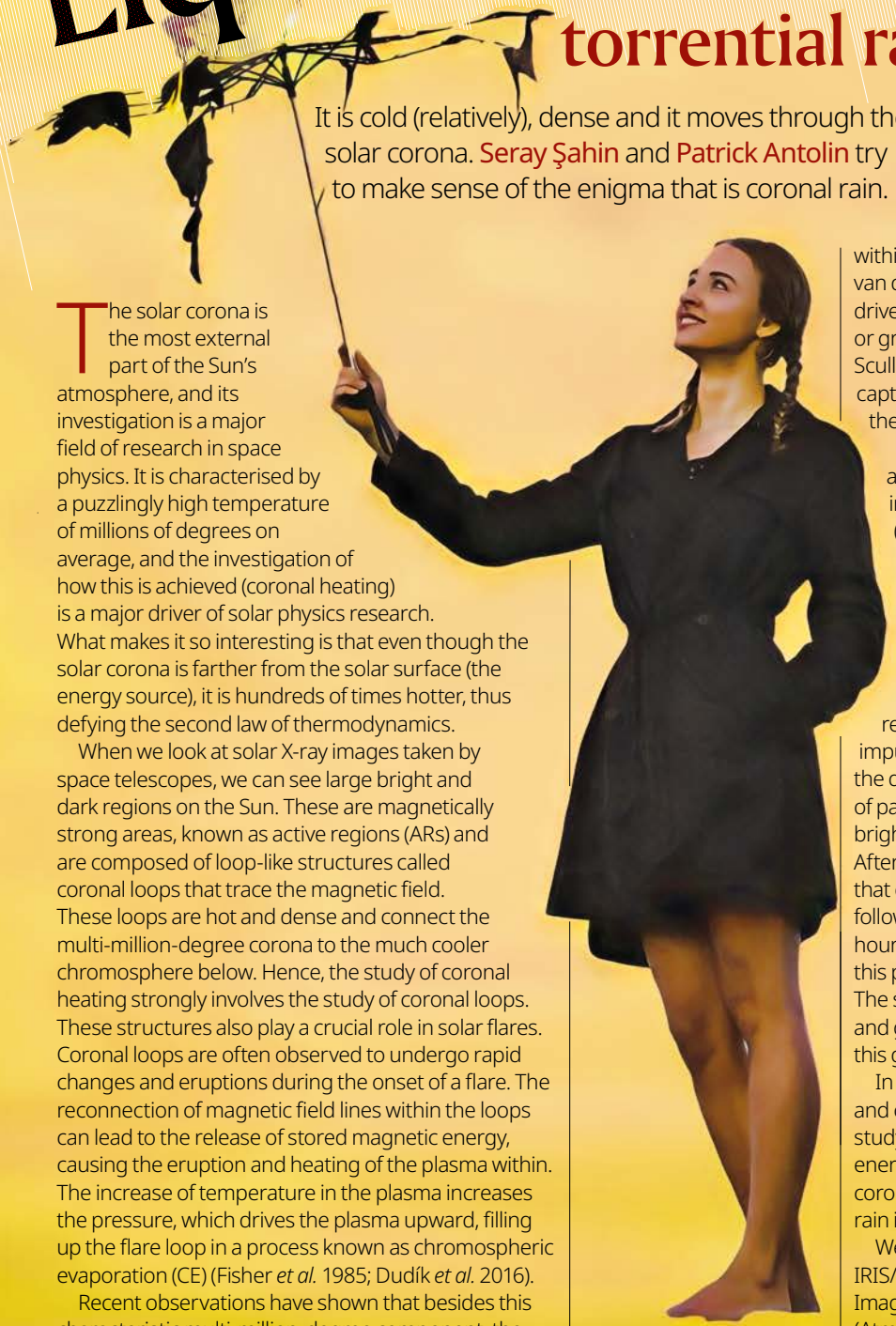

The solar corona is the most external part of the Sun's atmosphere, and its investigation is a major field of research in space physics. It is characterised by a puzzlingly high temperature of millions of degrees on average, and the investigation of how this is achieved (coronal heating) is a major driver of solar physics research. What makes it so interesting is that even though the solar corona is farther from the solar surface (the energy source), it is hundreds of times hotter, thus defying the second law of thermodynamics.

When we look at solar X-ray images taken by space telescopes, we can see large bright and dark regions on the Sun. These are magnetically strong areas, known as active regions (ARs) and are composed of loop-like structures called coronal loops that trace the magnetic field. These loops are hot and dense and connect the multi-million-degree corona to the much cooler chromosphere below. Hence, the study of coronal heating strongly involves the study of coronal loops. These structures also play a crucial role in solar flares. Coronal loops are often observed to undergo rapid changes and eruptions during the onset of a flare. The reconnection of magnetic field lines within the loops can lead to the release of stored magnetic energy, causing the eruption and heating of the plasma within. The increase of temperature in the plasma increases the pressure, which drives the plasma upward, filling up the flare loop in a process known as chromospheric evaporation (CE) (Fisher *et al.* 1985; Dudík *et al.* 2016).

Recent observations have shown that besides this characteristic multi-million-degree component, the corona also contains a large amount of coronal rain, material that is hundreds of times colder and denser than its surroundings. Coronal rain is a condensation phenomenon in the sense that material accumulates and catastrophically cools to thousands of degrees. The runaway cooling is driven by a thermal instability that is also invoked to explain cool structures at much larger scales in the universe, such as planetary nebulae in the interstellar medium and molecular clouds in the intracluster medium. Different kinds of coronal rain have been observed in the solar atmosphere (Antolin & Froment 2022), but the most common types are the 'quiescent coronal rain', which occurs within active region coronal loops (Antolin & Rouppe van der Voort 2012; Şahin *et al.* 2023), and the 'flare-driven coronal rain', which occurs after a solar flare or gradual phase (Bruzek 1964; Hara *et al.* 2006; Scullion *et al.* 2016; Şahin & Antolin, submitted). These captivating phenomena and the differences between the rain kinds are yet to be fully understood.

Solar flares go through three clearly defined stages as they develop over time: the pre-flare phase, the impulsive phase, and finally the gradual phase (Golub & Pasachoff 2009). During the pre-flare phase, small brightenings occur, which act as early indicators of a flare trigger, and includes events such as the emergence of new magnetic flux or filament activation. As magnetic fluxes interact, the systems can become unstable and erupt, thus releasing free magnetic energy through magnetic reconnection. This triggers a flare and begins the impulsive phase. The energy release that occurs due to the dissipation of magnetic fields and the acceleration of particles can be easily seen in the patterns of flare brightness across the electromagnetic spectrum. After the intense and rapid initial phase of a solar flare that can be as short as a few minutes, a slower phase follows, called the gradual phase, which can last for hours or sometimes extend to a day or more. During this phase, conductive and radiative cooling take place. The soft X-ray and EUV peak emissions are reached and gradually fade. Coronal rain is observed during this gradual phase and marks the end of the flare.

In our study, we investigate a C2.1-class flare and carry out the first high-resolution statistical study comparing the morphology, dynamics and energetics between quiescent and flare-driven coronal rain. We further investigate the role of the rain in the mass and energy cycle of the flare.

We used two space-based solar instruments, IRIS/SJI (Interface Region Imaging Spectrograph/Slit-jaw Imager described by De Pontieu *et al.* 2014) and AIA/SDO (Atmospheric Imaging Assembly/Solar Dynamics Observatory; see Pesnell *et al.* 2012; Lemen *et al.* 2012), spanning chromospheric (10^4K) to coronal (10^7K) temperatures. The rain is particularly well observed in the (IRIS) SJI 2796, (IRIS) SJI 1330 and AIA 304 channels, dominated, respectively by plasma emission at 10^4K, $10^{4.3}$K and 10^5K. Since coronal rain undergoes rapid morphological changes during its fall toward the solar surface, we need advanced methods to automatically detect and trace it. For this purpose, we used the 'Rolling Hough Transform (RHT)' technique tuned by Schad (2017) for rain and other solar applications.

Figure 1 shows the average radial velocity maps derived from the RHT routine for the pre-flare, impulsive

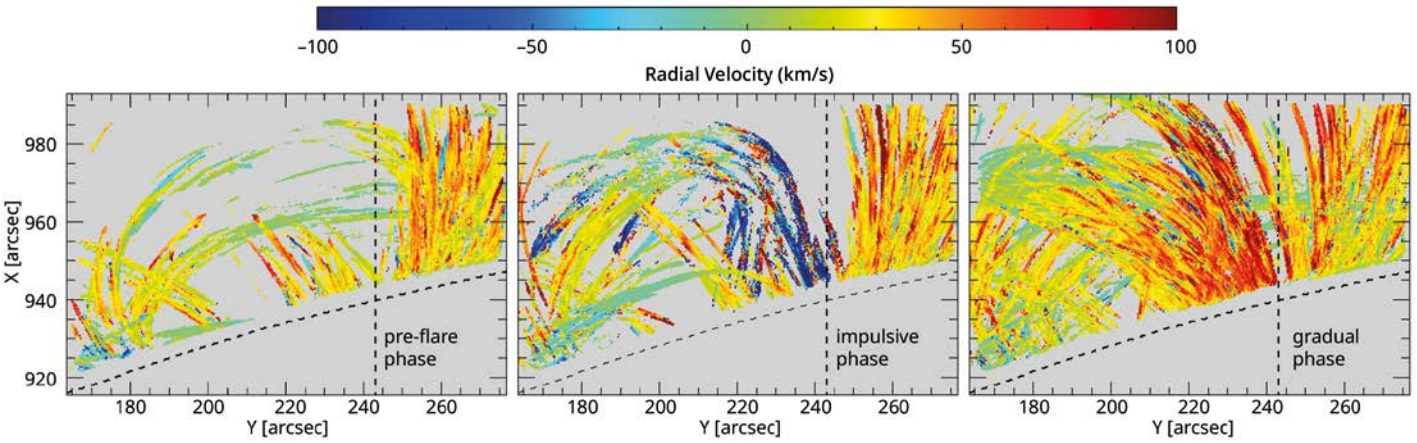

1 *Average radial velocity maps derived from the RHT over the pre-flare, impulsive, and gradual phases in SJI 1330. These maps indicate the dynamic change of coronal rain along the radial trajectory, with downward (positive values) and upward (negative values) motions. The solar limb is indicated by the dashed curve.* (S. Şahin)

and gradual phases in the SJI 1330 passband. As seen, coronal rain is widespread over the AR even before the flare, and it strongly increases in quantity from the pre-flare to the gradual phase. As expected from gravity, downward motions are much more dominant. In agreement with recent studies, the upward motions are also ubiquitous (Li *et al.* 2022; Şahin *et al.* 2023). While downflows correspond mainly to bulk flows that undergo acceleration as they fall, we found that upflow motions have higher velocities but are more stochastic and sporadic. Figure 2 shows the projected velocity distribution for each rain clump for downflows (top) and upflows (bottom) for the pre-flare and the gradual phases based on the left side of the vertical dashed lines in figure 1. As can be seen, downflow and upflow velocities have a broad distribution, up to 200kms^{-1}. The overall shape of the velocity distribution is very similar across the channels. The average median downflow velocity is 36±28kms^{-1} during the pre-flare phase and 50±38kms^{-1} for the gradual phase (a 39% average increase), with little difference across the channels. This velocity increase is probably due to an increase in rain density in which gas pressure forces and gravity compete (Oliver *et al.* 2014). However, the detailed rain kinematics are still a subject of investigation. It is still unclear why upflow speeds appear more stochastic and sporadic, but one reason could be the way cooling progresses. As the plasma rapidly cools and falls, it becomes more opaque, leading to apparent upward motions. Alternatively, as the rain falls the compression and heating of plasma ahead becomes stronger, which may lead to localised upward forces.

In figure 3, we show the SJI 2796 with spatial mean angle overlap (on the left panel). The spatial mean angle corresponds to the rain inclination angle with respect to the horizontal direction. On the right-hand side, we show the variation of detected rain pixels and corresponding intensities for each passband over the observational time. In response to the large release of energy, the amount of coronal rain in the gradual phase

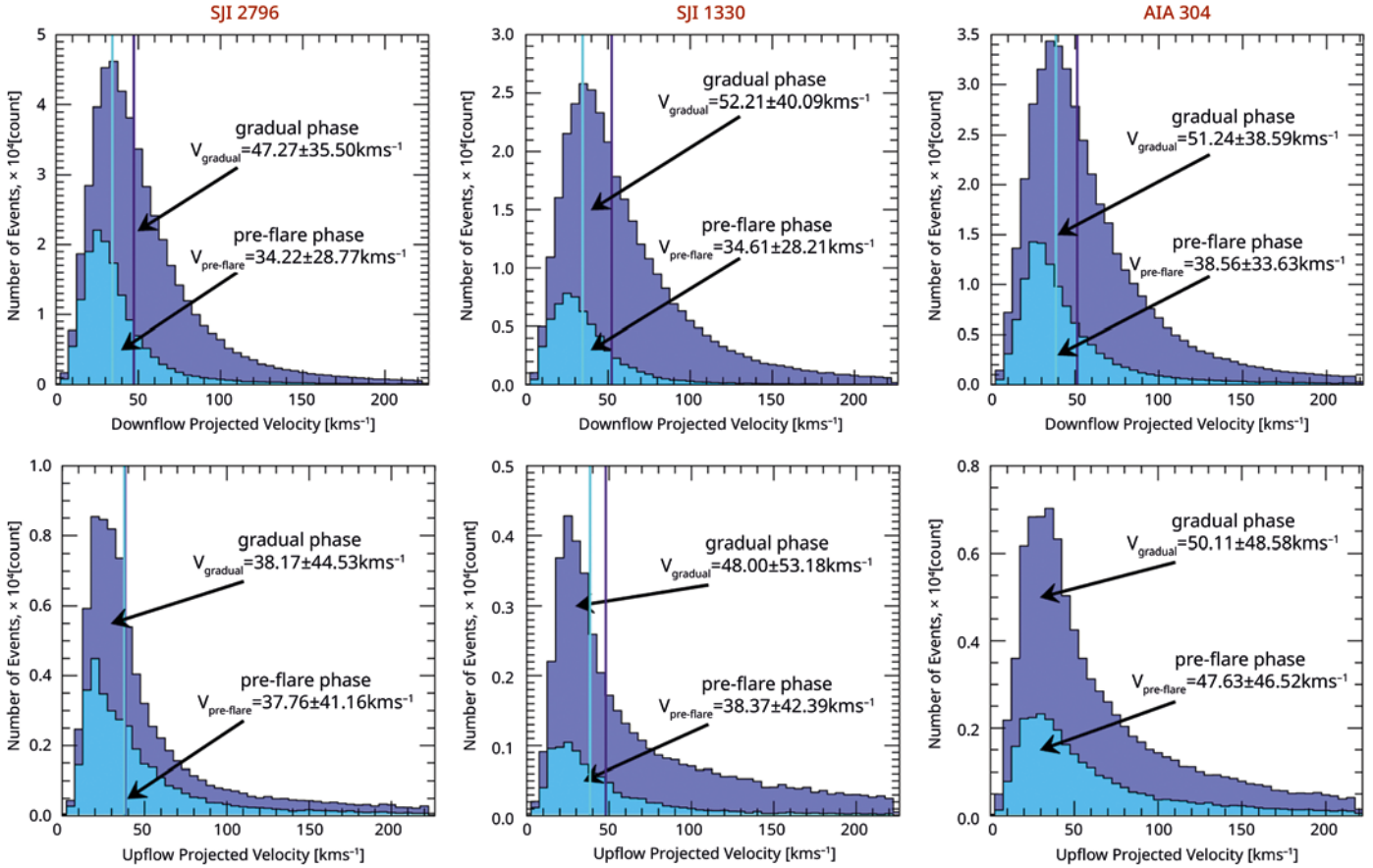

2 *Histograms of the projected velocity distributions during the pre-flare and gradual phases for the downflow (top) and upflow (bottom) motions in SJI 2796Å (left), SJI 1330Å (middle), and AIA 304Å (right), with the corresponding median and standard deviation in the inner caption.* (S. Şahin)

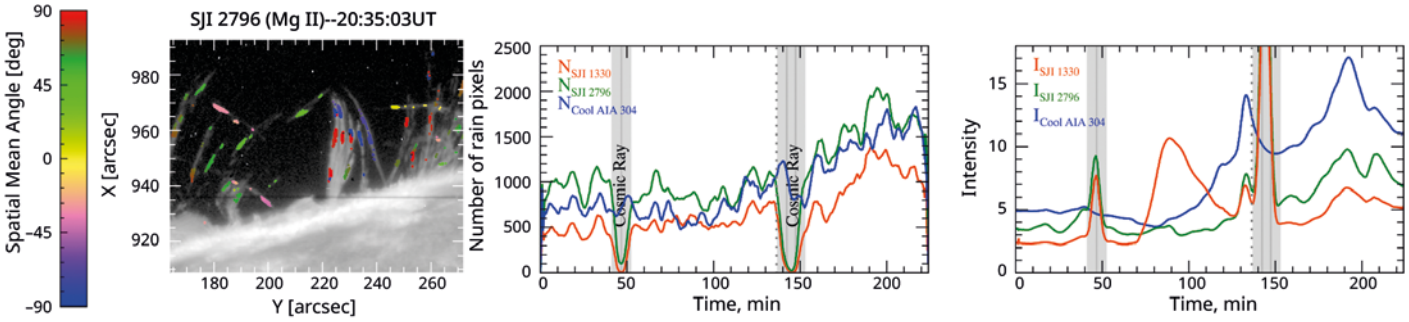

more than doubles compared to the pre-flare situation. Similarly, the intensity also increases from pre-flare to gradual phases. Specifically, the SJI 2796Å, SJI 1330Å, and Cool AIA 304Å show an increase of approximately 172%, 130%, and 252%, respectively. The differences in intensity are mainly associated with opacity differences between the dominating spectral lines. The strong temporal correlation across the channels, despite the differences in temperature formation, suggests a rapid cooling down to 10^4K, and also a clump morphology that ensures strong colocation in time and space of multi-thermal emission. This is likely the condensation corona transition region (CCTR), which is the thin boundary between the condensation and the corona and is expected to strongly emit in transition region temperatures (Antolin *et al.* 2022).

We also compared the width and length morphologies of the rain in pre-flare and gradual phases (see figure 4) and found that the average width remains essentially the same from pre-flare to gradual phases, despite the very strong changes in physical quantities introduced by the flare. This suggests that the rain width is set by a fundamental mechanism such as thermal instability in a way that is largely insensitive to the magnetic field strength. On the other hand, the average length is significantly increased during the flare. This may be simply because more material is produced at higher heights in the gradual phase.

Furthermore, we investigated the mass and energy cycle in the flare loop. The start of the cycle is marked by chromospheric evaporation during the impulsive phase (produced by the strong flare heating), while the end is marked by the rain showers in the gradual phase. Our estimations revealed that $5\pm2\times10^{13}$g are pushed upwards in the impulsive phase, while the estimated total mass going down in the form of rain is $4\pm0.004\times10^{14}$g in the gradual phase. This results in an average kinetic energy of $4.39\pm2\times10^{27}$erg for the chromospheric evaporation and $6.89\pm0.03\times10^{27}$erg for the rain. The one order of magnitude difference between the upflow and the downflow masses could be due to the fact that most of the material in the flare loop is probably becoming thermally unstable, with the resulting rain falling mainly towards the observed footpoint. Additionally, both footpoints are heated due to the flare, with the other footpoint outside of the IRIS field-of-view. However, this would imply a very large heating imbalance across footpoints, which is unlikely. Another possibility is the presence of additional and faster chromospheric evaporation at higher temperatures, outside of the range currently probed by the instruments. Next-generation spectrometers such as MUSE and EUVST (De Pontieu *et al.* 2022), will help elucidate this problem. Our results indicate that coronal rain plays a significant role in the mass and energy cycle between the chromosphere and the corona. ●

3 *SJI 2796 with spatial mean angle derived from RHT (left). Number of rain pixels (middle) and intensity (right) variation over time for the SJI 2796, SJI 1330, and Cool AIA 304. We applied an image processing technique (Antolin et al. in preparation) to separate the hot and cool component from AIA 304, since this passband includes mainly two temperature response peaks (He II 303.8Å at 10^5K and Si XI 303.32Å at $10^{6.2}$K).* (S. Şahin)

4 *1D Histogram distribution of rain clump widths (top) and length (bottom) for the pre-flare (left) and gradual phases (right).* (S. Şahin)

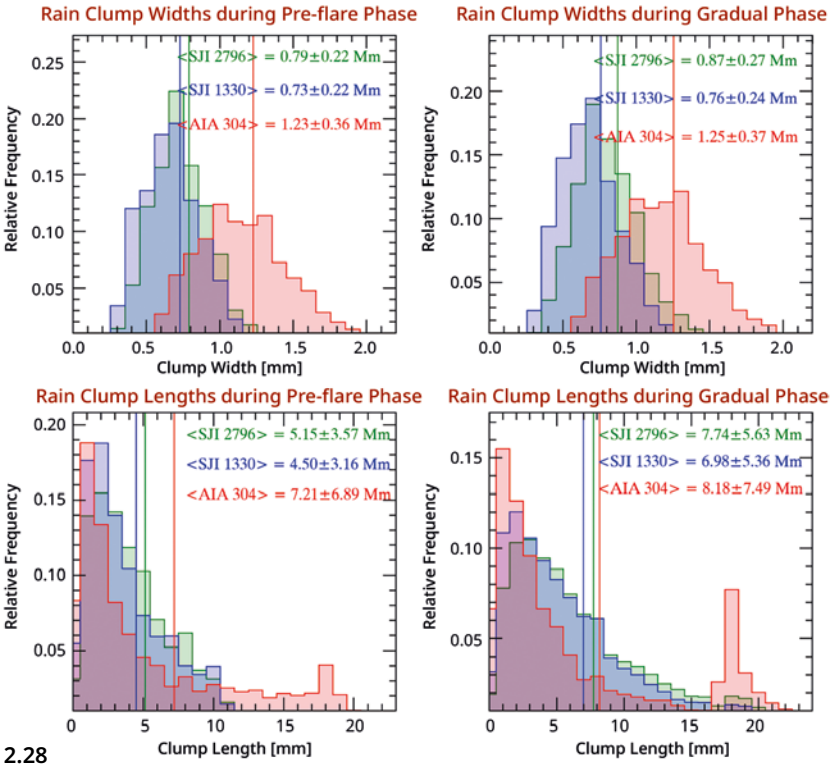

ACKNOWLEDGEMENTS

We are grateful to *A&G* for the opportunity to write this review and the UKSP ECR Team for the poster prize at NAM 2023. P.A. acknowledges funding from his STFC Ernest Rutherford Fellowship (No. ST/R004285/2). This research was supported by the International Space Science Institute (ISSI) in Bern, through ISSI International Team project #545 ('Observe Local Think Global: What Solar Observations can Teach us about Multiphase Plasmas across Physical Scales'). IRIS is a NASA small explorer mission developed and operated by LMSAL, with mission operations executed at NASA Ames Research Center and major contributions to downlink communications funded by ESA and the Norwegian Space Centre. SDO is a mission for NASA's Living With a Star (LWS) programme. AIA is an instrument on-board the Solar Dynamics Observatory. All SDO data used in this work are available from the Joint Science Operations Center (http://jsoc.stanford.edu) without restriction. This work has been submitted to *The Astrophysical Journal* under the title 'From Chromospheric Evaporation to Coronal Rain: An Investigation of the Mass and Energy Cycle of a Flare'.

AUTHORS

Seray Şahin (seraysahin93@gmail.com) recently received her PhD from Northumbria University. Outside of studying coronal rain, she enjoys exploring the wonders of Earth. With a passion for air sports, she firmly believes that 'It is always sunny above the clouds', symbolising not only her love for adventure but also her optimistic outlook.

Patrick Antolin (patrick.antolin@northumbria.ac.uk) is associate professor at Northumbria University. Besides his passion for astrophysics, he enjoys algebraic number theory, listening to techno and reading sci-fi books in the company of cats.

REFERENCES

Antolin P & Froment C 2022 *Front. Astron. Space Sci.* **9** 820116
Antolin P & Rouppe van der Voort L 2012 *Astrophys. J.* **745** 152
Antolin P *et al.* 2022 *Astrophys. J. Lett.* **926** L29
Bruzek A 1964 *Astrophys. J.* **140** 746
De Pontieu B *et al.* 2014 *Sol. Phys.* **289** 2733
De Pontieu B *et al.* 2022 *Astrophys. J.* **926** 52
Dudík J. *et al.* 2016 *Astrophys. J.* **823** 41
Fisher GH *et al.* 1985 *Astrophys. J.* **289** 414
Golub L & Pasachoff JM 2009 *The Solar Corona CUP*
Hara H *et al.* 2006 *Astrophys. J.* **648** 712
Lemen JR *et al.* 2012 *Sol Phys* **275** 17
Li X *et al.* 2022 *Astrophys. J.* **926** 216
Oliver R *et al.* 2014 *Astrophys. J.* **784** 21
Pesnell WD *et al.* 2012 *Sol Phys* **275** 3
Şahin S *et al.* 2023 *Astrophys. J.* **950** 171
Schad T 2017 *Solar Phys.* **292** 132
Scullion E *et al.* 2016 *Astrophys. J.* **833** 184